LOW COST NUCLEAR THERMAL ROCKET CERMET FUEL ELEMENT ENVIRONMENT TESTING

D.E. Bradley, O.R. Mireles, R.R. Hickman
Nuclear Systems, NASA Marshall Space Flight Center
Huntsville, AL

ABSTRACT

Deep space missions with large payloads require high specific impulse and relatively high thrust to achieve mission goals in reasonable time frames.[1,2] Conventional storable propellants produce average specific impulse. Nuclear thermal rockets capable of producing high specific impulse are proposed. Nuclear thermal rockets employ heat produced by fission reaction to heat and therefore accelerate hydrogen, which is then forced through a rocket nozzle providing thrust. Fuel element temperatures are very high (up to 3000 K), and hydrogen is highly reactive with most materials at high temperatures. Data covering the effects of high-temperature hydrogen exposure on fuel elements are limited.[3] The primary concern is the mechanical failure of fuel elements that employ high-melting-point metals, ceramics, or a combination (cermet) as a structural matrix into which the nuclear fuel is distributed. The purpose of the testing is to obtain data to assess the properties of the non-nuclear support materials, as-fabricated, and determine their ability to survive and maintain thermal performance in a prototypical NTR reactor environment of exposure to hydrogen at very high temperatures. The fission process of the planned fissile material and the resulting heating performance is well known and does not therefore require that active fissile material be integrated in this testing. A small-scale test bed designed to heat fuel element samples via non-contact radio frequency heating and expose samples to hydrogen is being developed to assist in optimal material and manufacturing process selection without employing fissile material. This paper details the test bed design and results of testing conducted to date.

INTRODUCTION

The mechanical failure of fuel elements exposed to hydrogen at very high temperatures is a high risk liability to the successful implementation of Nuclear Thermal Rockets (NTRs).[1,2] The fissile nuclear material used in such fuel elements to generate a very high heating density requires a stable support matrix that is robust enough to persist in the presence of flowing hydrogen at temperatures as high as 3000K. Thus, test candidate materials without the inclusion of fissile nuclear materials are proposed to reduce the great expense of nuclear infrastructure during early testing. Such a study will leverage existing research to narrow the field of likely material candidates and then exercise frequent test iterations to focus on the best materials and manufacturing practices. With this knowledge, fuel elements may then be fabricated to include fissile material for prototypical testing in a reactor environment. However, without the thermal energy generated by the nuclear fuel, an alternative for non-contact volumetric heating of fuel elements during testing is required. Radio frequency (RF) heating fulfills both of these requirements and is proposed for low-cost testing of candidate materials. The first goal of this testing hardware is to demonstrate that prototypical reactor temperatures up to 3000K can be achieved in the fuel samples predictably and reliably using RF heating. The physical inclusion of flowing hydrogen is considered to be a secondary goal and strictly dependent on the successful completion of RF heating system development. Plans are in progress to integrate these two major design features while invaluable operational hardware testing takes place.

RESULTS AND DISCUSSION

PRACTICAL GOALS OF TESTING

1. Achieve and maintain as high a temperature as possible in a sample fuel element (up to 3000 K).
2. Flow hydrogen through the heated element while attempting to maintain the fuel element at temperature.
3. Remove fuel element after testing and conduct materials characterization and mechanical testing to determine effects of hydrogen on element at high temperatures.

---

4. Using the resulting materials properties data, adjust the manufacturing process, material feedstock contents, and fuel pin geometry for new fuel elements and then repeat testing.
5. Identify knowledge gaps in data and devise tests to fill them.

MAJOR TEST HARDWARE CHALLENGES

1. Achieve, maintain, and measure high temperature of sample fuel element.
2. Safely expose fuel element to known quantity of flowing hydrogen.
3. Achieve a rapid turnaround between fuel element tests.

METHODS OF SAMPLE HEATING CONSIDERED

Several methods of heating representative fuel element samples were considered prior to the buildup of this test hardware. A very basic understanding of how a prototypical NTR system operates provides some insight into what is desired in a non-nuclear test.

Ideally, nuclear fuel is evenly distributed and suspended within a high temperature-resistant support matrix. Fission releases heat throughout the volume of the fuel element as opposed to on exposed surfaces. Hydrogen gas passes over the outer surface of the fuel element and absorbs the heat released by fission. In order to maximize the surface area available for the convection heat transfer from the fuel element to the hydrogen, flow channels within the fuel element may be incorporated. This energy transfer has a very high power density which ultimately makes it appealing for in-space applications. For the purposes of this testing we therefore wanted very high power density, volumetric heating and the ability to monitor fuel element temperature.

Electrical power is readily available in the research environment and it remains only to determine what mechanism of conversion most closely mimics that of nuclear fission cost-effectively as described above. Two major mechanisms were considered: resistance heating and RF heating.

1. Resistance heating is well understood, commonly used and power supplies are readily available. Resistance heating requires very close proximity if not direct contact to the object being heated. This in turn requires the use of special high-temperature resistant materials in order to achieve temperatures of 3000 K. Two different techniques for using resistance heating were considered.
    a. The use of the fuel element as a resistance heating element requires electrical conductors that are capable of operation while in direct contact with the element, but provides the best possible visibility of the fuel element during test to allow non-contact pyrometric temperature measurement.
    b. The use of a box-shaped resistance heating element into which the fuel element is placed does not place electrical conductors directly in contact with the fuel element, thus reducing the need for very high temperature resistance, however supporting the element in such a box would increase complexity and the box would also block visibility required by pyrometry. The materials required to fabricate such a box would also be potentially reactive in a hydrogen atmosphere making it potentially less robust over the long term.

2. RF heating involves the use of relatively expensive power supplies producing tuned frequencies of alternating current provided by high power solid state semiconductors. While substantially more expensive than conventional resistance heating power supplies, RF power supplies are becoming more common due to their use in industry for automated, non-contact heat treatment of metal parts produced in large quantities. These power supplies are therefore robust and also semi-customizable for heating of different sizes and types of parts. Another advantage of RF heating is zero physical contact with the fuel element reducing the need for high-temperature resistant conductors. Heating coils can also be custom-made to allow visible access to the fuel elements for pyrometry.

RATIONALE FOR SELECTED TEST HARDWARE

A full scale test simulating the environment of a nuclear thermal rocket has been in development over the past several years at NASA-MSFC known as the Nuclear Thermal Rocket Element Environmental Simulator or NTREES.[2] NTREES utilizes RF heating and as a result, there was an obvious advantage to selecting test hardware leveraging experience gained with that experiment. In addition, a low-cost system capable of simple, sub-scale operation as described in this report is a direct investment in operational knowledge and hardware experience required for continued development of a full scale system.

Existing research hardware used previously in other non-nuclear fission power systems and materials testing was available to assemble the hardware described in this report. Because of the system's overall similarity to the full-scale NTREES and the availability of existing research hardware, an RF heating system deployed in a vacuum chamber was selected. Sub-scale hardware was also used to simplify the rapid turnaround studies of component changes such as coil configurations and fuel sample insulators. Finally, hardware operational experience was readily obtained with a small-scale system due to the very low operating expenses. This experience provided the necessary background experience to assess and evaluate RF heating system designs, to understand and fully capitalize on non-contact temperature measurement via pyrometry, and to understand thermodynamic characteristics and relevant governing equations of the system.

TEST HARDWARE SETUP

The test hardware used a very small custom-fabricated vacuum chamber 10 in. in diameter by 18 in. tall that was capable of vacuum levels up to 10E-6 Torr. The chamber was integrated with the RF heating system via a vacuum-rated RF power feed-through.

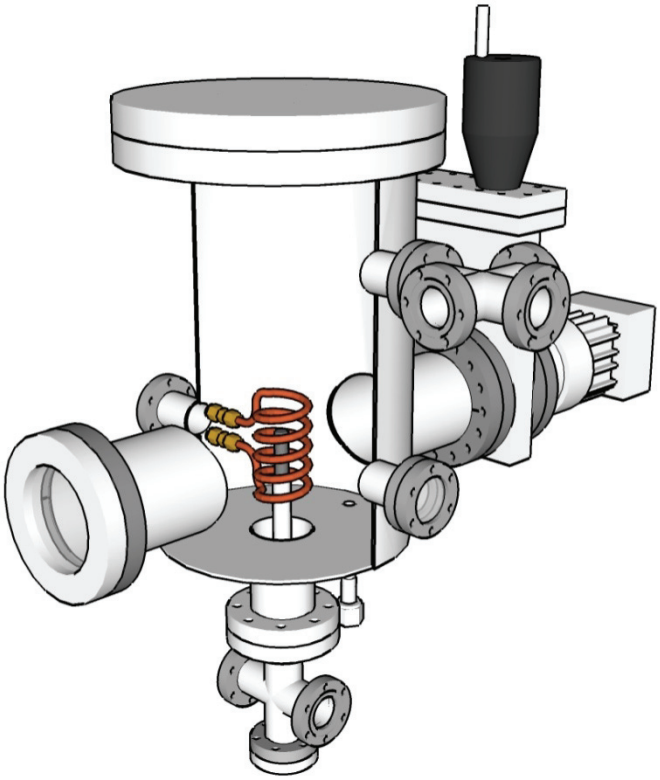

Figure 1. CFEET (Cermet Fuel Element Environment Test) baseline configuration CAD model.

The RF heating coil was located inside the vacuum chamber and was powered by a 15 kW Flexitune, water-cooled RF power supply connected with copper tubing. The copper tubing functioned as both the water-cooling channel and the electrical current conductor. Cooling water was circulated throughout the components within the RF power supply and also flowed through the RF heating coil itself. Heat was rejected from the RF coil and power supply cooling water to the building's facility cooling water using a water-to-water heat exchanger. The vacuum chamber reduces heat loss from the fuel element due to convection heat transfer and maintains an environment that precludes arcing of the RF coil.

Arcing can be caused by the ionization of any gases surrounding the RF coil which creates a lower-resistance flow path for the applied RF power.[3] The tendency to arc is best described by a Paschen curve which takes into account gas properties (type and pressure), the physical proximity of conductors to one another between which arcing can occur, and the voltage of the applied electric power. In general, for a given proximity of conductors, higher voltages are more likely to result in arcing than lower voltages and a there is a critical, sub atmospheric gas pressure at which the tendency to arc is a maximum. A Paschen curve for atmospheric air is provided for reference below.

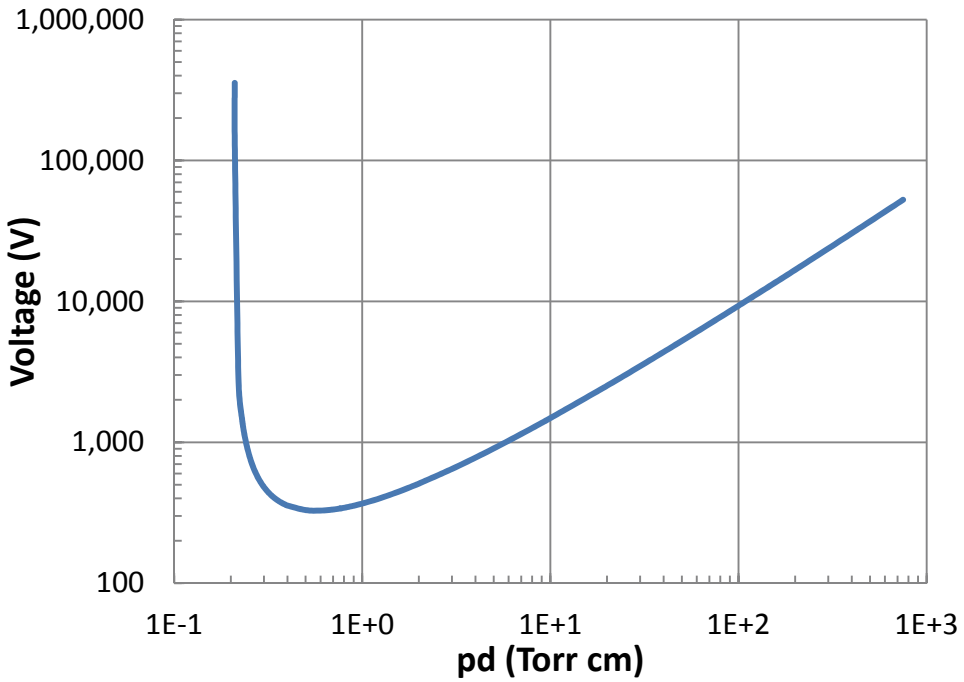

Figure 2 - Paschen Curve for Air

The test setup was based on fabrication simplicity rather than overall best thermal efficiency. The fuel element to be heated was simply supported by a pedestal made of boron nitride, a ceramic with a melting (sublimation) point of 2973 °C. No flowing hydrogen gas was employed at this stage of testing, and as such, no other parts came in physical contact with the sample element.

The fuel element was supported simply at the center of the RF coil and positioned along its axial centerline so that a clear line-of-sight existed to pyrometers outside the vacuum chamber.

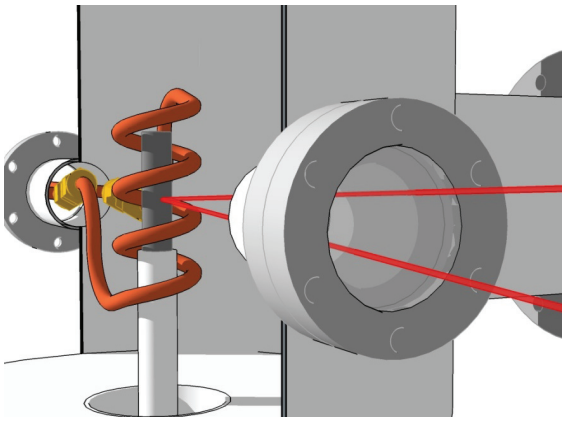

Figure 3. Fuel element support detail showing pyrometer lines of sight and RF coil.

VACUUM CHAMBER

The vacuum chamber was originally built for performing high-temperature-materials compatibility verification testing for the Jupiter Icy Moons Orbiter (JIMO) program.[4] Testing was intended to take different materials and bonding techniques and observe their performance when subjected to a working fluid of Helium and Xenon in accelerated-life testing consisting of higher-than-normal temperatures, impurity concentrations, and thermal cycling.

The vacuum chamber was fabricated from a 10-in-diam 304 stainless steel tube oriented vertically. A single 10-in.-diam Conflat™ flange at the top of the chamber provided physical access to any in-chamber hardware, including the RF heating coil for adjustments and replacement. Two 6-in.-diam Conflat flanges were positioned across from each other near the bottom of the chamber. A single 4-in.-diam Conflat flange at the bottom of the chamber provided access to the fuel element sample with minimal chamber disassembly. Several 2.75-in. Conflat flanges were available for roughing pump connection, vacuum measurement, and optical flanges for pyrometer use.

RF POWER SUPPLY

The RF power supply was a 15kW Flexitune™ model 2-255750-001 solid state converter.

Figure 4. Flexitune +15, 15kW, 20-60 kHz RF power supply.

It operated at an output frequency of 20–60 kHz at 150 V (2400 A). The output power was user-adjustable down to a minimum of 10% of maximum power, or 1500 W. For power levels below 1500 W, a custom circuit was designed to provide on/off cycling of power at user-selectable intervals to simulate duty cycle fractions below 100%.

WATER-TO-WATER HEAT EXCHANGER

The water-to-water heat exchanger was a custom PolyScience™ recirculator model LL70. It incorporated a water pump that cycled conductivity-controlled water through the RF power supply and back to a heat exchanger, where heat was rejected to the building's facility cooling water.

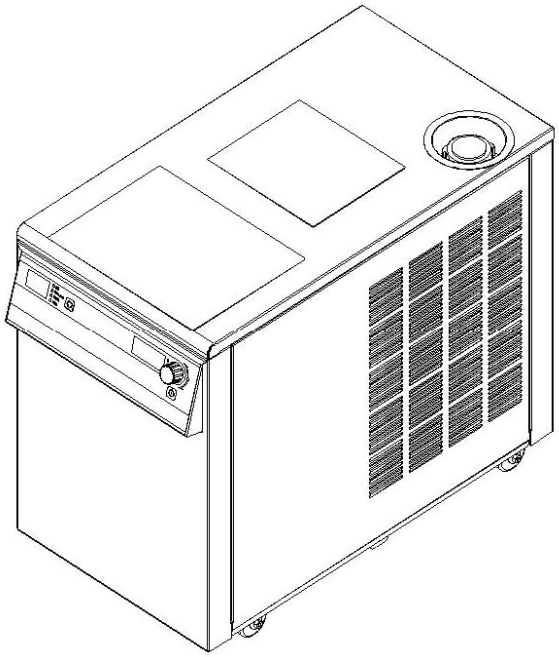

Figure 5. Polyscience recirculating water-to-water heat exchanger.

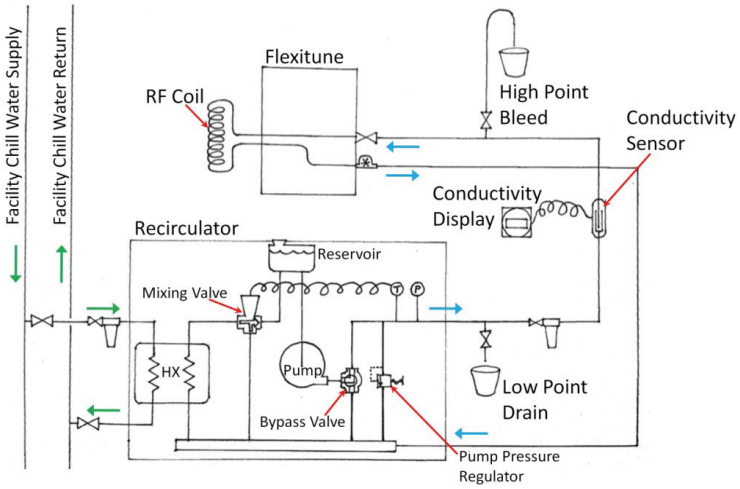

Figure 6. Cooling water flow schematic.

RF COILS

The RF coils were hand-turned from bendable copper refrigeration tubing to appropriate dimensions for testing. Dimensions typically required a trade-off between RF operating frequency and enclosed fuel element dimensions.

Figure 7. Hand-turned RF heating coil, 3/8-in.-diam tubing.

In order to minimize development time and cost, detailed coil design analysis was minimized. Coils may be carefully designed analytically to maximize heating efficiency and compatibility with a given power supply and part configuration. In this hardware setup, a coil would be turned to a have a certain diameter, number of turns and pitch (spacing between turns) without regard to optimization. Once installed, testing provided insights into overall efficiency and suitability of the coil design. Adjustments were made to subsequent coils and so on in an iterative fashion.

If an RF coil combined with the power supply at a resonant frequency outside of the operating range of the power supply, tuning capacitors were added or removed as necessary to provide minor adjustments. If adjustments to the tuning capacitance failed to bring the resonant frequency within the operating range of the power supply, the RF coil geometric properties were changed. Typically, this amounted to turning a new coil and adjusting the number, spacing, and diameter of the turns.

A simple spiral wound coil has an inductance given by the following equation:

$$L = \frac{\mu_0 \mu_r N^2 A}{l}$$

where L is the inductance (Henry), μ_0 is the permeability of free space ($4p \times 10^{-7}$ H m^{-1}), μ_r is the relative permeability of core material, N is the number of turns, A is cross-sectional area of the coil (m^2), and l is the length of coil (m).

The conductor geometry leading to the coil affected the overall inductance of the circuit. For the purposes of estimating operational frequencies, the non-coil geometric effects were ignored. It was assumed that shifts in frequency up or down based only on changes to the RF coil geometry would result in a similar shift in operational frequency. Because RF coils are relatively simple to fabricate and quite complex to model numerically, this solution allowed the rapid turnaround of coil design to focus on target frequencies.

The resonant frequency of a capacitor/inductor circuit is given by the following equation:

$$f = \frac{1}{2\pi\sqrt{LC}}$$

where f is the frequency (Hz), and *C* is the capacitance (Farad).

In general, greater fuel element heating depth was obtained with lower frequencies. Therefore, to achieve volumetric heating more typical of a nuclear fuel element, lower frequencies were desired. At extreme limits of the power supply frequency range, however, power limiting can occur. The best-case scenario for maximum available heating power was to operate at the middle of the power supply's design frequency range. Therefore, for the purposes of this testing, the RF coils were fabricated so that a resulting operating frequency between 20 and 40 kHz was obtained.

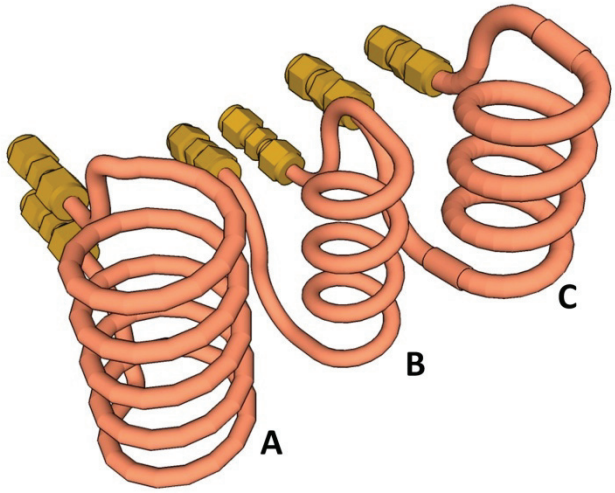

Figure 8. Different coils installed for testing.

Table 1. RF heating coil dimensions and estimated operating frequencies.

Coil	Tube Size, in.	Coil Diameter, in.	Number of Turns	Length of Coil, in.	Calculated Inductance, μH	Estimated Resonant Frequency, kHz	Operating Frequency as Tested, kHz
A	0.250	2.000	5	4	0.51	27.4	21.2
B	0.250	1.250	4	4	0.14	52.4	25.0/28.8*
C	0.375	1.875	4	4	0.29	36.4	Future work

* Operating frequency change (improvement) due to addition of bus bars on RF tubing.

The RF coils were positioned very close to the fuel element to be tested and were therefore subjected to very high thermal radiation. At high fuel element temperatures, the rate of heat loss from the fuel element to the RF coil may exceed the ability of the cooling water to extract the heat and maintain power output. Additional water flow can be achieved by increasing water pressure or increasing RF coil tubing cross-sectional area. In practice, coils were fabricated using 0.25 in diameter tubing. Vacuum chamber feedthroughs available for this application are available for both 0.25 and 0.375 in diameter tubing. An upgrade in cross sectional area to 0.375 in diameter tubing is underway.

INSTRUMENTATION

TEMPERATURE MEASUREMENT

Because the very high part temperatures desired and expected from this testing configuration, physical contact with these parts was not practicable. Optical pyrometry, which is a viable method for non-contact measurement of fuel element temperature, was used.

OPTICAL PYROMETER PRINCIPLE OF OPERATION

A pyrometer produces an output signal based on the intensity of incident radiation at the specific wavelengths for which the pyrometer is designed.[5] With a known surface emissivity less than 1.0 (grey body), temperature can then be directly solved for by using the Stefan–Boltzmann law for grey bodies:

$$j^* = \varepsilon \sigma T^4$$

where j^* is the irradiance, energy per time per area, (W/m^2); ε is the emissivity (ε = 1 for perfect blackbody); σ is the Stefan-Boltzmann constant (5.6704 × 10^{-8} J s^{-1} m^{-2} K^{-4}), and T is the temperature of measured body (K).

Two separate pyrometers were employed for testing: a Mikron™ M770S, two-color pyrometer and a FAR™ multi-wavelength pyrometer.

DATA ACQUISITION SYSTEM

Two low-cost USB data acquisition cards were used to record relevant data channels as summarized in table 2.

Table 2. Data acquisition channels.

USB Data Acquisition Card	Channel	Measurement Range	Signal Type
DATAQ, DI-145	RF Power	0kW – 15kW	±10VDC
	RF Frequency	20kHz – 60kHz	±10VDC
	Mikron Pyrometer	600 °C – 1400 °C	±10VDC
	FAR Pyrometer	800 °C – 1500 °C / 2000 °C – 4000 °C	±10VDC
OMEGA, USB-4718	Fuel Element Pedestal Temp 1	−200 °C to +1350 °C	Type K TC
	Fuel Element Pedestal Temp 2	−200 °C to +1350 °C	Type K TC
	Fuel Element Pedestal Temp 3	−200 °C to +1350 °C	Type K TC

In addition to these channels, the FAR pyrometer was equipped with its own data-logging capability, including temperature, tolerance, and emissivity, based on recording the full spectrum of incident light intensity data between wavelengths of 455 to 972 nm.

As of this writing, a single data acquisition system is planned which will envelope the above channels and add several additional channels. It is expected that more data describing the RF power input, several more thermocouples, and the vacuum quality in the vacuum chamber will be recorded during subsequent testing.

THERMODYNAMIC MODEL

Thermal energy was supplied to the fuel element via RF heating and was lost by thermal radiation and thermal conduction. The thermal conduction loss took place at the interface between the fuel sample and the boron nitride fuel sample support pedestal. The fuel sample “saw” both the RF coil and the vacuum chamber wall in ratios defined by the geometry of the RF coil. The emissivity of the fuel sample changed as it went through a wide range of temperatures, whereas the emissivity of both the RF coil (copper) and the vacuum chamber wall (stainless steel) was relatively constant due to their approximately isothermal conditions.

As thermal radiation is proportional to the fourth power of temperature difference and conduction to the first, thermal radiation losses dominated, particularly as higher fuel element temperatures were achieved.

Therefore, to achieve maximum fuel element temperatures, the effective system emissivity was required to be reduced by means of reflectors or other view-factor-reducing methods.

TEST RESULTS

MELTING TEST

After preliminary checkout testing, which confirmed operation of the RF power supply and basic functionality of the optical pyrometers, a melting test using a 308 stainless steel dummy sample was performed. The melting point of 308 stainless steel is approximately 1500 °C and this known property acted as a general functional/calibration point for the pyrometers. Pyrometer temperature measurements were observed in parallel with visual observation of the dummy sample. With melting observed by sight, RF power was discontinued and pyrometer output temperature recorded.

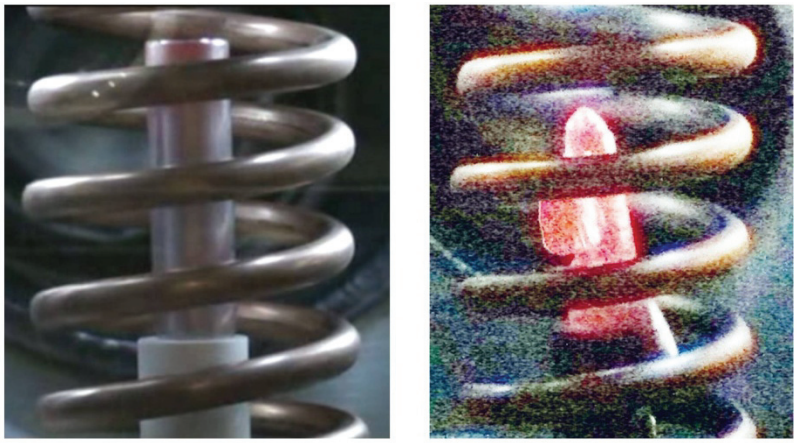

Figure 9. 308 stainless steel sample before and after melting at 1500°C.

A rough estimation of overall RF heating efficiency based on raising the sample temperature from 25°C (room temperature) to 1500°C (sample melting point) is shown in Table 3.

Table 3. Estimated Overall RF Heating Efficiency Calculation for 308 Stainless Steel Sample

Value	Variable Description and Units
50	duration of applied RF, s
9.3	power output level indicated on Flexitune, kW
465	total energy input, kJ
25	start temperature, °C
1500	end temperature, °C
500	specific heat, Cp, J/kg·K
8.03	density, ρ, g/cm^3
6.44	sample volume, V, cm^3
51.67	sample mass, m, g
38.11	total energy added to fuel element, kJ
8.2	Overall efficiency of RF heating, %

LOW-POWER HEATING TESTS

To achieve the maximum possible fuel element temperatures, some effort was made to reduce radiation heat transfer from the fuel element to the vacuum chamber wall. That loss mechanism was the primary heat loss path. Two different techniques were investigated: 1) the use of a reflecting shield inside the vacuum chamber and outside the RF coil, and 2) the use of a high temperature ceramic insulator located between the RF coil and the fuel sample.

A following baseline heating test was used to compare the effectiveness of different heat loss reduction schemes. The RF power supply supplied 1.5 kW for each test, heating a 308 stainless steel sample to 1200°C or a steady state temperature, whichever was lowest. This resulted in a recorded heating profile and subsequent cooling profile that was visually compared, test to test, to provide qualitative results.

A radiation reflector fabricated out of niobium sheet metal was installed around the outside of the RF coil. During initial tests, substantial thermal deformation of the shield was observed. The close proximity of the conductive shield to the RF coil caused heating of the shield, and it was apparent that higher heating loads would damage the shield and potentially short out the RF coil. As a result, radiation reflector testing was discontinued pending a suitable shield redesign.

Testing proceeded using an aluminum oxide ceramic insulator installed around the sample fuel element, between the sample and the RF coil. The alumina insulator was cut from stock-tube-shaped material and a small port was machined to allow pyrometers to “view” the heated part.

Figure 10. Alumina Insulator installed around fuel element inside 1.875-in.-diam RF coil.

Data were recorded for four separate tests: 1) heating sample at 1.5 kW without insulation, vacuum pumps isolated; 2) heating sample at 1.5 kW with insulation, vacuum pumps isolated; 3) heating sample at 1.5 kW with insulation, vacuum pumps operating; and 4) heating sample at 1.5kW without insulation, vacuum pumps operating.

The heating profile shown in figures 11 and 12 clearly indicates that, for the temperature regime of 600–1000 °C, no appreciable gain in heating efficiency is obtained by the inclusion of a ceramic insulator between the RF coil and the fuel element. In addition, these figures underscore the importance of fully baking out ceramics prior to use; the release of volatiles upon heating is shown in the dotted line, which varies considerably during heating when compared to the other three tests.

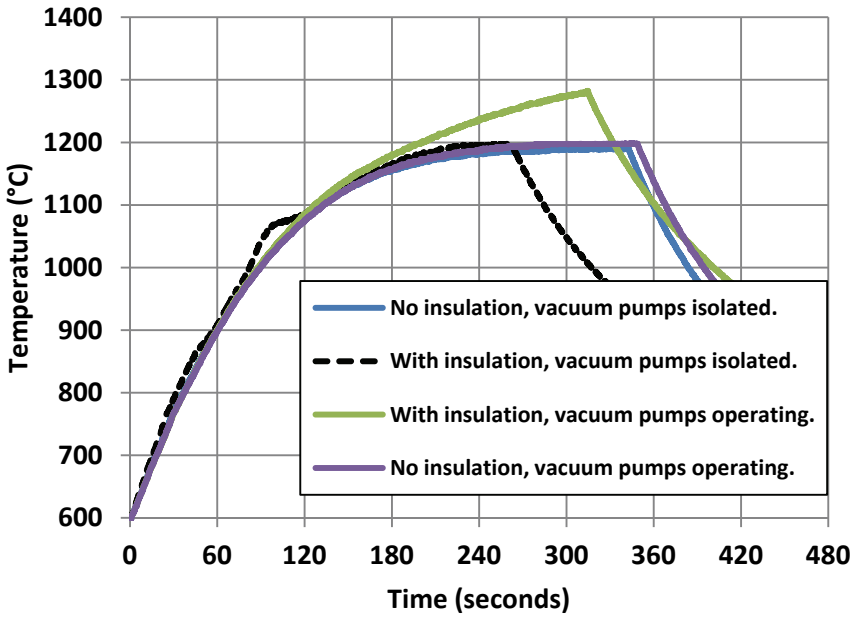

Figure 11. Fuel element temperature profile during low-power heating tests, 600 °C to maximum.

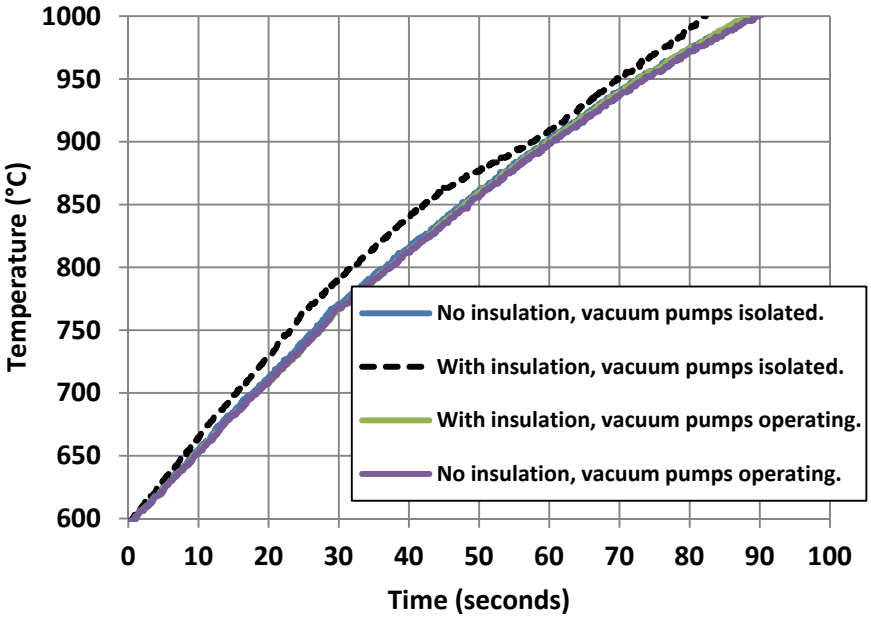

Figure 12. Fuel element temperature profile during low power heating tests, 600–1000 °C.

With the fuel element at higher temperatures, the effectiveness of the insulator can be seen in the figure 13. In both cases in which an insulator was used, the rate of heat loss was noticeably reduced. It should also be noted that, as the quality of vacuum dropped (as was the case when the vacuum pumps were isolated), a greater heat loss rate resulted.

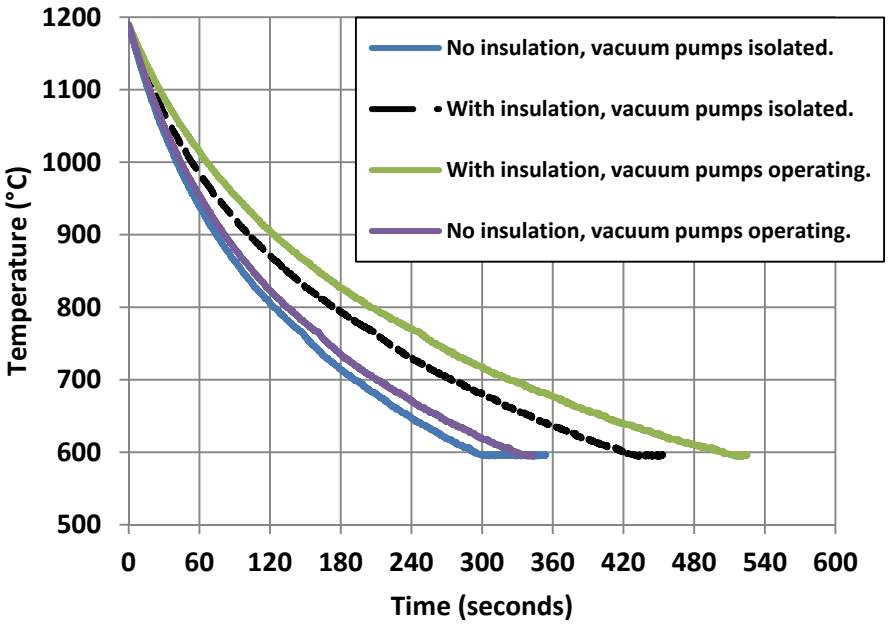

Figure 13 - Fuel element temperature profile during low-power cooling, approx. 1200–600 °C.

The best results for maximum heating were therefore obtained by maintaining the deepest possible vacuum and using an insulator between the RF coil and the fuel sample.

HIGH-POWER HEATING TESTS

The test hardware was subjected to maximum RF power operation, operating on a high-temperature surrogate fuel element sample. The sample was a cermet material consisting of hafnium nitride particles dispersed in a tungsten/rhenium alloy matrix with the following properties:

W: Tungsten, 63% by weight, Cp=132 J/Kg·K, MP=3422 °C
Rh: Rhenium, 5% by weight, Cp=136 J/Kg·K, MP=3186 °C
HfN: Hafnium Nitride[6], 32% by weight, Cp≈249 J/Kg·K, MP= 3305 °C
Sample Mass: 92.881 g
Estimated properties (based on mass percentages): Cp=169.8 J/Kg·K, MP=3373 °C
Dimensions: ½ in. in diameter x 1.5 in. in length
Sample Density: 19.2 g/cm^3

The results of low-power testing indicated the use of a high-temperature ceramic insulator between the fuel element sample and the RF coil. A zirconium dioxide ceramic insulator was fabricated by machining a plastic mold for casting. The insulator was designed to be a close fit to the inner diameter of the RF coil while leaving sufficient clearance to the fuel element to allow for its thermal expansion.

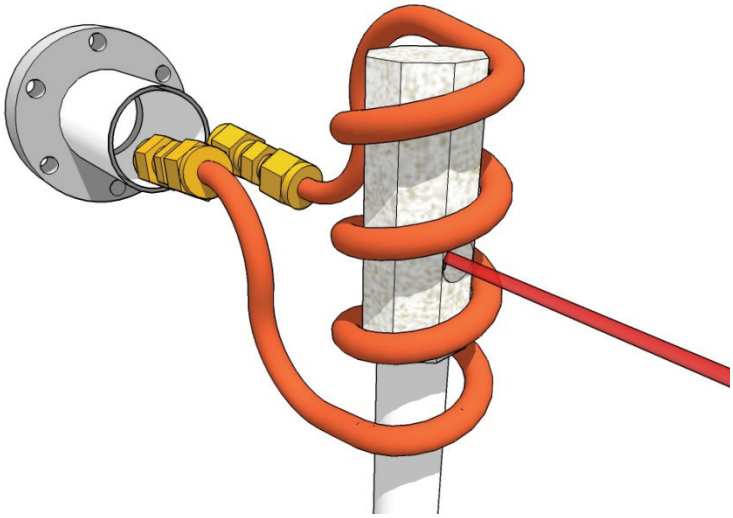

Figure 14. Hardware setup for high-power test with zirconia insulator.

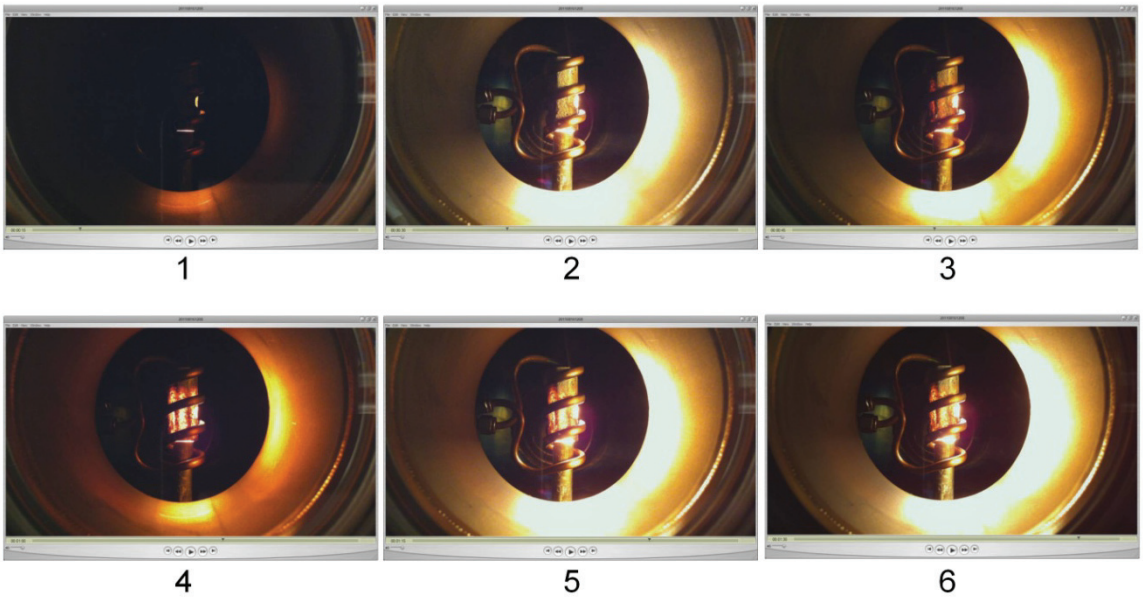

Figure 15. High-power heating test, 15-s intervals showing coil and insulator.

The RF heating system operated at 15 kW at a frequency of 28.8 kHz for the high-power tests. Figure 15 shows the temperature profile of the fuel element sample during the test. The RF power supply was automatically tripped off due to cooling water temperatures exceeding a hardware limited set-point. This temperature limit was hardware set to 40 °C. When the power tripped off, the cooling water temperature dropped below 40 °C in about 60 s (as shown in the figure) and allowed heating to resume. A maximum fuel element temperature of 1931 °C was recorded during the test.

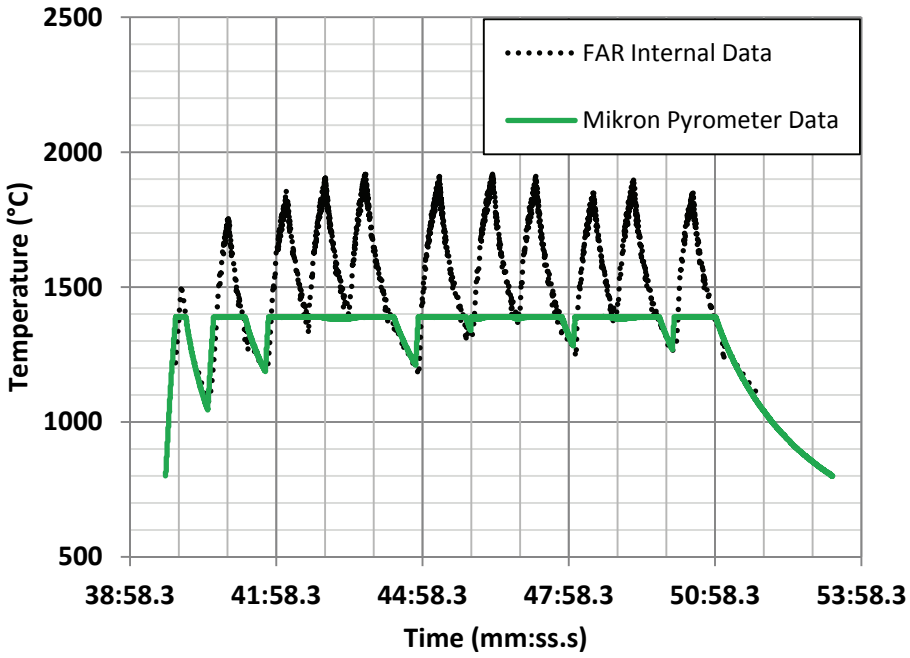

Figure 16. Fuel element temperature profile during high-power test.

The range limitations for the two different pyrometers are demonstrated in the figure 16. The Mikron unit was at saturation (maximum value) at 1400 °C, whereas the FAR unit was unable to measure temperatures below about 1100 °C.

The test setup was visually explored. There were two major sources of cooling water heating: 1) direct thermal radiation from the heated sample to the copper RF coil, and 2) conduction to the RF coil via the ceramic insulator. The coil was adjusted so that the view factor, defined as the proportion of all that radiation which leaves surface A and strikes surface B, between the fuel sample and the coil was effectively zero (no direct line of sight). This change did not alter system performance. As a result, it was concluded that the ceramic insulator, once sufficiently heated, was physically conducting heat to the RF coil as it had several contact points due to a close fit.

Figure 17. In-coil zirconia ceramic insulator and high-temperature fuel element after high-power testing.

It is important to note that the operational temperature limit achieved in this test was not due to a limitation of the RF power supply but rather a limitation of the cooling water system.

SUMMARY AND CONCLUSIONS

These initial series of tests have demonstrated that RF heating in a vacuum is a viable method for obtaining volumetric heating in proposed NTR fuel element samples up to 1900 °C. Non-conductive, high-temperature ceramic insulators installed between fuel element samples and an RF heating coil provides a significant performance advantage over uninsulated samples in terms of maximum achievable temperature at a fixed input power level.

FUTURE WORK

It is expected that an upgrade to the water cooling capacity will allow significantly higher achievable fuel element temperatures in future experiments. The overall cooling capacity can be increased by reducing the incoming cooling water temperature and increasing the volumetric flow rate through the system. A refrigerated water recirculator with the same footprint as the water-to-water heat exchanger is available and will be substituted into the system to provide for a lower net cooling water inlet temperature. The water pumping capacity available in the system is fixed by pump curve; a larger flow cross-sectional area or less overall system resistance is required to obtain a higher flow rate. Upgrading all of the RF copper tubing from ¼ in. in diameter to 3/8 in. in diameter, assuming a relative reduction in pressure drop throughout the flow path, will provide additional water flow.

A new RF coil turned from 3/8-in.-diam copper tubing will provide the opportunity to design an improved, ceramic in-coil fuel element insulator. The new insulator will be designed to have zero physical contact with both the fuel element and the RF coil, thereby reducing heat leak. In addition, the new insulator will be a two-piece design, which should reduce thermal stresses that led to cracking of the single-piece insulator.

Because of the number of physical changes required to facilitate an increase in cooling water flow, the test hardware is undergoing an upgrade. This includes modification of the data system. The upgraded system is expected to be operational at the end of the calendar year.

ACKNOWLEDGMENTS

The authors would like to acknowledge the following people: Jim Martin, for his encouragement, technical insight and for providing access to the appropriate equipment for test setup; Boise Pearson, for his assistance in identifying experienced personnel working similar testing; Dr. Bill Emrich, for providing technical information relating to the larger NTREES test project and for providing high-temperature material resources; Ricky Dickens, for assisting with technical discussions regarding the advantages and disadvantages of different electrical heating techniques and high-temperature material selection; Robert C. Goldstein and Christopher J. Yakey, for their technical guidance with regard to optimizing RF heating design; Ralph A. Felice for expertise in deploying pyrometry for non-contact temperature measurement and last but not least, Diana LaChance, for her assistance in writing, editing, and preparing this document.

REFERENCES

1. Bruno, C.: ***Nuclear Space Power and Propulsions Systems***, Volume 225, Progress in Astronautics and Aeronautics, AIAA, Reston, VA (July 2008).

2. Emrich, W. J.: ***Nuclear Thermal Rocket Element Environmental Simulator (NTREES)***, NASA 20080015668, Marshall Space Flight Center, Huntsville, AL, (February 2008).

3. Meek, J. M.; Craggs, J. D.: ***Electrical Breakdown of Gases***, New York, NY: John Wiley & Sons, Ltd. (1978)

4. Jet Propulsion Laboratory, California Institute of Technology: ***JUPITER ICY MOONS ORBITER (JIMO) an element of the Prometheus Program Annual Report***, 982-R06933, JPL 04-016 10/04, Pasadena, CA, (October 2004).

5. Felice, R. A.: ***The Spectropyrometer – a Practical Multi-wavelength Pyrometer***, Presented at the 8th Symposium on Temperature: Its Measurement and Control in Science and Industry, (October 2002).

6. Gupta, S. D.; Gupta, S. K.; Jha, P. K.: ***High pressure study on the phonon spectra and thermal properties in hafnium nitride and zirconium nitride***, Journal of Thermal Analysis and Calorimetry, Online First™, (June 2011)